Tuesday, October 14, 2003
Afternoon Session II
GEOLOGY OF THE MARTIAN NORTH POLAR LAYERED DEPOSITS *(Continued)*
3:45 p.m. Victoria Room

Milkovich S. M. * Head J. W. III
North Polar Cap of Mars: Correlation of Layers Within and Between Troughs **[#8082]**

Pathare A. V. * Paige D. A.
The Sublimation and Relaxation of Troughs and Scarps Within the Martian North Polar Layered Deposits **[#8087]**

PANEL DISCUSSION
THE MARTIAN POLAR LAYERED DEPOSITS: THE ROLE OF MELTING AND FLOW
Panelists: TBD

GENERAL DISCUSSION

NORTH POLAR CAP OF MARS: CORRELATION OF LAYERS WITHIN AND BETWEEN TROUGHS.
S. M. Milkovich and J. W. Head, III, Department of Geological Sciences, Brown University Box 1846, Providence, RI, 02912. Sarah_Milkovich@brown.edu

Introduction: Layered deposits exist within the northern residual cap of Mars exposed on the walls of the dark lanes or troughs seen cutting into the cap (Figures 1 and 2). These deposits consist of extensive lateral layers of ice and dust and are found throughout the polar cap. They were first identified in Mariner 9 images [1, 2] and later studied in detail with the Viking orbiters [e. g. 3, 4, 5, 6]. Recent images from Mars Global Surveyor show that the layers have a range of thicknesses and albedos, and are not continuous throughout the cap [7, 8]. Formation theories regard the layers as products of climate change due to orbital cycles [9, 4, 5], similar to climate changes caused by Milankovitch cycles on Earth [10], although the details of the formation processes remain unknown.

Characterization of the layered deposits is key to understanding the details of the layer formation process as well as understanding the processes which shape the polar regions and the martian climate as a whole. This study quantitatively correlates layers in images in order to assess variations within the layered deposits. Such variations can provide constraints for layer formation; for example, how widespread and how uniform is layer deposition on an individual layer scale, and how well do layers correlate within and between troughs?

Method: Many studies of terrestrial climate change are in the field of paleoceanography. Thus, we have adapted a paleoceanographic technique for studying correlations and variations between ocean drill cores. By matching distinctive shapes in the data sets under examination, one can establish correlations and then see how much one data set (the signal) needs to be adjusted to look like the other data set (the target). In this way, one can get a sense of the correlations and changes in accumulation rate between the two sites. By adapting this method to study the stratigraphy of the polar layered deposits we are able to assess correlations and get a sense of the variations between two location within the cap.

Profiles of grayscale intensity, or digital number (DN), taken from MOC images are compared using Match 1.0, a program developed by Lisiecki and Lisiecki [11] to compare sets of paleoceanographic data. This program uses dynamic programming to minimize the square of the differences between the data sets in order to adjust one data set to fit as close as possible to the other set. This method has been used to compare changes in δ^{18}O values down a core at multiple locations; we use it to compare changes in DN value down a trough wall at multiple locations. In this way, it is possible to measure quantitatively how similar two stratigraphic sequences are.

Prior to comparing profiles from two images, the images must be calibrated and corrected for the slope of the trough wall. To do so, images are calibrated and the associated MOLA data retrieved using programs from the ISIS image processing package. The MOLA data is interpolated between shots to provide an elevation value for each pixel of the image. Thus, the exposure of layers in the image is projected back onto the vertical wall of the trough. The DN profile is then adjusted to run perpendicular to the layer margins. In this way, the data from an overhead image is adjusted to be more like the data from a core sample perpendicular to the cap surface. The profiles are also normalized before they are run through Match 1.0; this entails subtracting the mean from each series and then dividing by the standard deviation. Thus, the data series for each profile will have a mean of 0 and a standard deviation of 1, which improves the ability of Match 1.0 to compare similar data series.

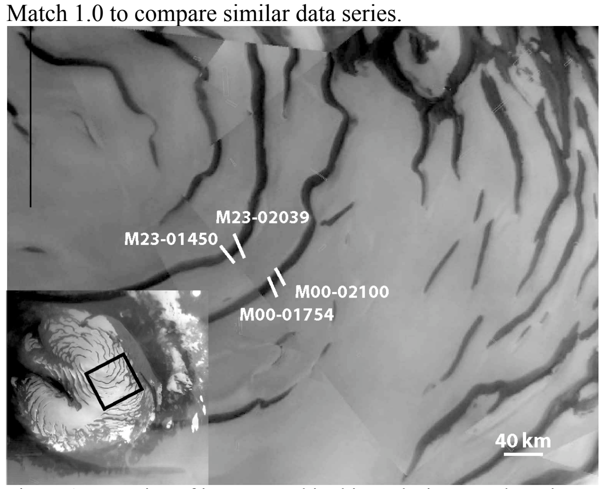

Figure 1. Location of images used in this analysis. Inset box shows location within the cap.

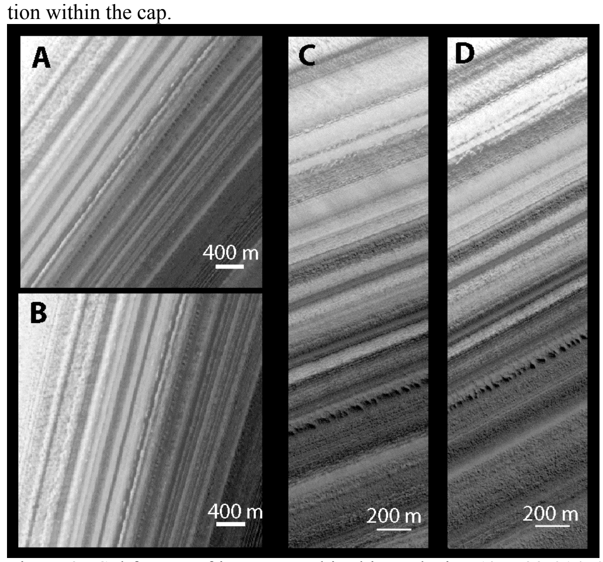

Figure 2. Subframes of images used in this analysis. A) M23-01450. B) M23-02039. C) M00-01754. D) M00-02100. Illumination from the upper right in all images.

The four images selected for this analysis (Figure 2) were taken in the same Ls range (northern summer) to minimize the effects of seasonal frost. M00-01754 and M00-02100, from the southern trough, both have resolutions of 1.8 m/pxl while M23-01450 and M23-02039 have resolutions of 12.1 m/pxl.

Results: Figures 3, 4, and 5 show the results of the matching analysis. In each figure, the top graph shows the normalized, corrected profiles plotted with depth before being matched. The signal is the DN profile which was adjusted to match the target DN profile. The middle graph in each figure plots the results of the matching analysis. The bottom graph shows how much the signal needed to be adjusted along the profile to match the target; this is in essence a relative net accumulation rate (NAR). If no adjustment was necessary, the relative rate is 1.

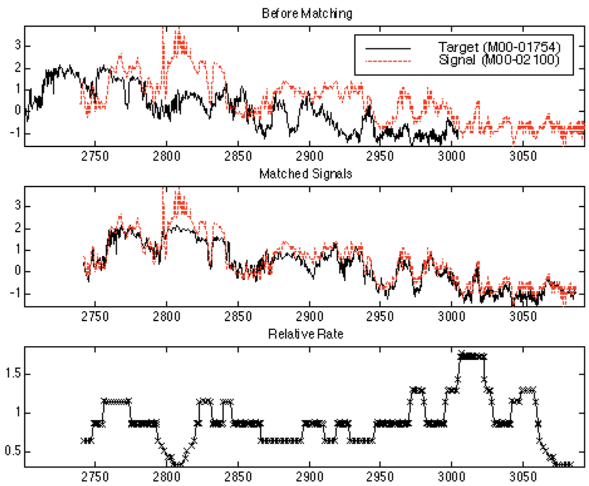

Figure 3. Results of matching M00-01754 and M00-02100. The coefficient of determination (r^2) for this match is 0.9036; 90.36% of the variation in the datasets is related. This indicates a good match between the datasets.

The preliminary results of this analysis are 1) that there is reasonable good correlation between layers in different areas of one trough and between troughs, and 2) that the accumulation rate along a trough varies considerably. Images M00-01754 and M00-02100 are about 18 km apart, and the NAR varies between them up to a factor of two. Additionally, the NAR does not increase systematically – at times one location has the higher NAR while at other times the other location has the higher rate.

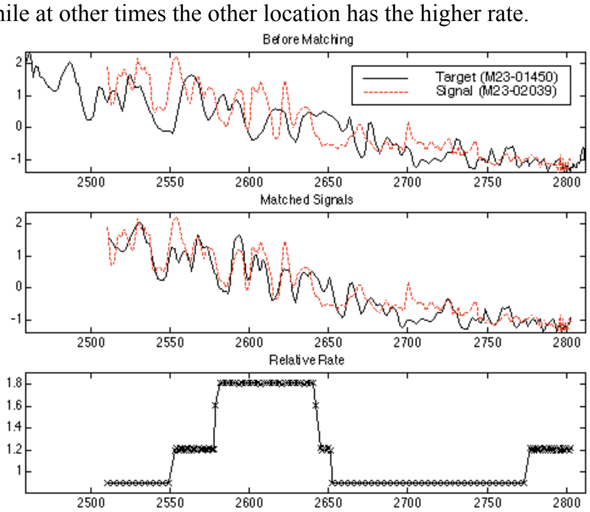

Figure 4. Results of matching images M23-01450 and M23-02039. The coefficient of determination (r^2) for this match is 0.8619; 86.19% of the variation in the datasets is related. This indicates a good match between the datasets.

Additionally, the net accumulation rates do not change in the same manner between the two troughs. The relative rates between M00-01754 and M00-02100 are very different than those between M23-01450 and M23-02039. This implies that there is a great deal of local variation in the layer accumulation process. This can clearly be seen in Figure 5, in which an image from each trough is compared. There is good correlation between the two troughs, with relative accumulation rates again below 2. But the shape of the relative rate curve is different from the relative rate curves of the comparisons of images within a single trough.

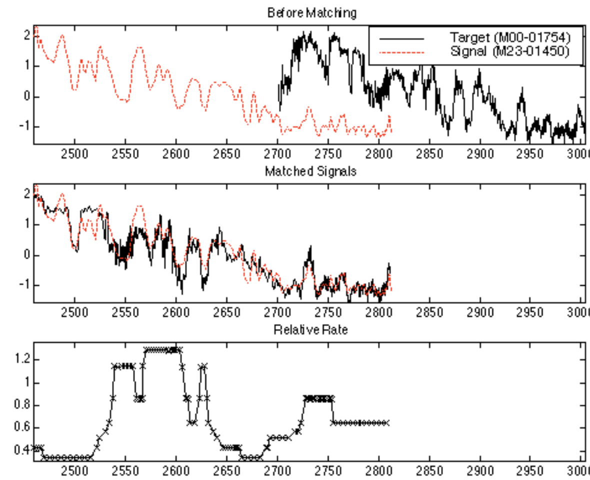

Figure 5. Results of matching M00-01754 and M23-1450. The coefficient of determination (r^2) for this match is 0.8965; 89.65% of the variation in the datasets is related. This indicates a good match between the datasets.

Discussion. Laskar et al [12] examined M00-02100, one of the images used in this study. They compared cycles identified in the image with calculated insolation cycles to find NAR for this area. For the top 250 m the calculated NAR was 0.05 cm/yr. Below that the NAR slowed to 0.025 cm/yr. In order to test these results, it is necessary to determine if these rates remain reasonable for the region. Based on our matching analysis, we find that the DN profile from this image is quantitatively comparable to the three other images in this study. Therefore, under this set of assumptions it is possible to extrapolate NAR to the rest of the region.

The relative rates between the images remain within a factor of 2; therefore, the NAR for this region should be between 0.025 and 0.1 cm/yr for the uppermost section of the region. Estimates of the resurfacing rate for the north polar region based on cratering rates have values as high as 0.1-0.2 cm/yr [13], so the variations on the Laskar et al values are within current estimates. Further studies within this region of the polar cap are required to see if the rates remain plausible.

The fact that the profiles correlate well between two troughs indicates that layers are deposited over a large area, greater that just one trough. However, because the relative rates are not constant, this deposition is not uniform; nor does it change systematically between images or between troughs.

Acknowledgements: The authors gratefully thank Tim Herbert and Lorraine Lisiecki for helpful discussions and assistance with the computer programs.

References: [1] Soderblom, L. A., M. C. Malin, J. A. Cutts, and B. C. Murray.(1973) *J. Geophys. Res.,78,* 4197-4210. [2] Cutts, J. A., (1973) *J. Geophys Res., 78*, 4231-4249. [3] Kieffer, H. H., et. al, (1976) , *Science, 194*, 1341-1344. [4] Blasius, K. R., J. A. Cutts, and A. D. Howard (1982) *Icarus, 50*, 140-160. [5] Howard, A. D., J. A. Cutts, and K. R. Blasius.(1982) *Icarus 50*, 161-215. [6] Thomas, P. et al, (1992) In *Mars*, H. H. Kieffer et al ed. Univ. of Arizona Press. [7] Malin M. C. and Edgett K. S. (2001) *J Geophys Res, 106*, 23429-23570. [8] Milkovich, S. M. and J. W. Head (2001) *LPSC 32* , 1976. [9] Squyres, S. W. (1979) *Icarus 40*, 244-261. [10] Imbrie, J. (1982) *Icarus 50*, 408-422. [11] Lisiecki, L. E. and P. A. Lisiecki (2002) *Paleoceanography, 17*, art no. 1049. [12] Laskar, J. et al. (2002) *Nature, 419*, 375-377. [13] Herkenhoff, K. and J. J. Plaut. (2000) *Icarus 144,* 243-253.

THE SUBLIMATION AND RELAXATION OF TROUGHS AND SCARPS WITHIN THE MARTIAN NORTH POLAR LAYERED DEPOSITS.

A. V. Pathare[1] and D. A. Paige[2]. [1]Division of Geological and Planetary Sciences, California Institute of Technology (avp@gps.caltech.edu), [2]Dept. of Earth and Space Sciences, University of California, Los Angeles, CA (dap@ucla.edu).

Summary: The kilometer-scale topography of the North Polar Layered Deposits (NPLD) is dominated by troughs and scarps: Fig. 1 shows both (a) the ubiquity of troughs throughout the NPLD, and (b) the enhanced steepness of scarps at the margins of the NPLD (e.g., along the inner wall of the channel-like reentrant, Chasma Boreale). Although the surface slopes and total depths of NPLD troughs and scarps are widely presumed to result from surface ablational processes, here we propose that an alternative mechanism, viscous relaxation of subsurface water ice, governs the morphological evolution of NPLD troughs and scarps.

Topography: Using the 64 pixel/degree MOLA altimetry grids, we constructed eight radial profiles spaced at 45° longitudinal intervals through the North Polar Dome. Along each profile, we have identified all interior troughs and marginal scarps with depths greater than 200 m located between 80°N and 87°N. Fig. 2 plots maximum 1.6-km baseline surface slopes observed along the equatorward-facing (EWF) walls of troughs and scarps, as well as upon the poleward-facing (PWF) walls of troughs.

As previously noted [1], most NPLD troughs are asymmetric: our measurements (Fig. 2A) indicate that maximum EWF slopes (α_ε) are on average 75% steeper than maximum PWF slopes (α_ρ). Although primary scarps at the periphery of the NPLD are generally at least twice as steep as interior troughs, we find that there is no significant dependence of trough slope (Fig. 2A) or depth (not shown) upon latitude. Interestingly, the slopes and depths of NPLD troughs and scarps are strongly correlated with one another (Fig. 2C).

Sublimation: The most widespread theories of PLD evolution [1,2] presume that the asymmetrical slopes of most NPLD troughs ($\alpha_\varepsilon > \alpha_\rho$) result from preferential H_2O sublimation from EWF trough walls. However, our modeling indicates that there is no long-term sublimation advantage of EWF trough walls, due to the effects of obliquity upon the slope dependence of sublimation rate (Fig. 3). We define a parameter R comparing the sublimation rates from the mean EWF and PWF trough wall slopes of α_ε = 5.4° and α_ρ = 3.1°, respectively; at the present obliquity (θ = 25.2°), the relative sublimation ratio R = 1.33.

However, the sublimation enhancement of EWF slopes is limited to lower obliquities, since as obliquity increases and the average solar zenith rises, the benefit of being tilted towards the sun close to local noon is

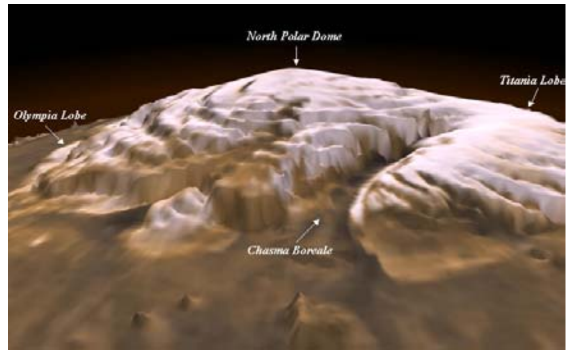

Fig. 1. Overlay of an NPLD Viking image mosaic upon MOLA topography, created by the GSFC Scientific Visualization Studio and the MOLA Science Team. Vertical exaggeration ~ 300x.

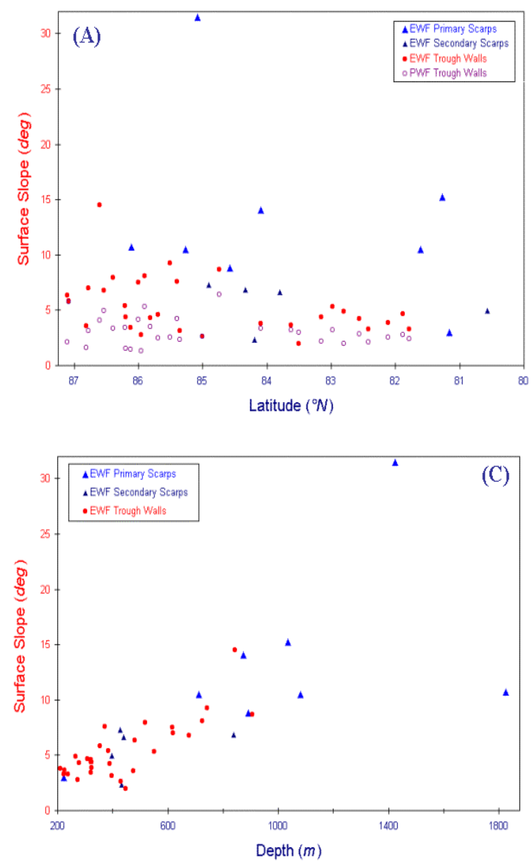

Fig. 2. Dependence of the maximum surface slopes of NPLD trough and scarp walls upon (a) latitude and (c) depth. Surface slopes are calculated over an approximate 1.6-km baseline.

offset by the disadvantage of being tilted away from the sun during the now brighter nighttime hours. Thus at obliquities of θ = 32.1° / 37.5° / 45.0°, the relative sublimation ratio R = 1.06 / 1.00 / 0.98. (Note that sublimation is actually slightly enhanced from PWF trough walls at near-maximum obliquities).

Since 80% of NPLD sublimation over the last 10 Myr takes places at obliquities above the median θ = 32.1°, our calculations demonstrate that EWF trough wall sublimation, when integrated over an obliquity "cycle", is not much greater than that from PWF trough walls (R = 1.02 since t = 10 Ma). Hence we conclude that, contrary to expectations, the steeper EWF slopes of NPLD trough walls do not result from long-term preferential sublimation driven by insolation variations.

Relaxation: But then what causes the slope asymmetry of opposing trough walls? We propose that viscous relaxation of subsurface water ice—which we have previously shown to be important to South PLD crater morphology [3]—may also govern NPLD trough and scarp evolution. Although [2] suggested that the continued presence of troughs argues against PLD flow, our trough simulations of NPLD troughs with the finite element model Tekton [4] predict trough closure times of approximately several million years.

Furthermore, Fig. 4 shows that if the EWF half of the trough is just 2 K warmer than the PWF half—which is consistent with the slope-dependent temperature variation over the last few Myr predicted by our subsurface thermal modeling—then maximum EWF slopes will become significantly steeper than maximum PWF slopes (Fig. 5), due to the slower rate of uplift of the inner PWF trough walls (which can be attributed to the increased subsurface viscosity below the colder PWF slopes). Additionally, we show that relaxation of NPLD trough and scarps can readily account for the correlation of surface slope and total depth (Fig. 2C), an observation that is particularly difficult to explain via sublimation or eolian erosion.

Conclusions: (1) The slope asymmetry of PLD troughs does not result from preferential sublimation but rather from differential relaxation of opposing trough walls. (2) Present-day NPLD troughs have formed since 5 Ma, and are not sites of long-term deposition. (3) Glacial flow probably governs the large-scale evolution of the North PLD.

References: [1] Thomas P. *et al.* (1992) in Mars, Ed. H. Kieffer *et al.*, Univ. Arizona Press, Tucson, 767-795. [2] Clifford S. *et al.* (2000) *Icarus* **144**, 210-242. [3] Pathare A. V. *et al.* (2002) *LPSC XXXIII*, Abstract #1972. [4] Melosh H. J. and Raefsky A. (1980) *Geophys. J. Royal Astron. Society* **60**, 334-354.

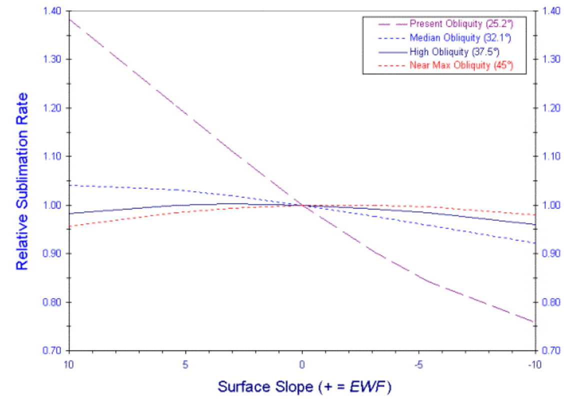

***Fig.** 3*. Dependence of sublimation upon EWF surface slope, expressed relative to the net annual sublimation rate at α_ε = 0°, for four different obliquities and nominal North PLD conditions.

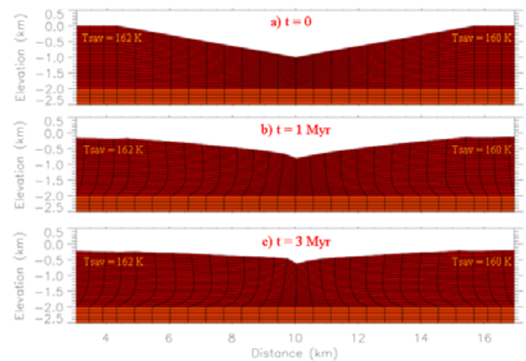

Fig. 4. Relaxation history at time steps of t = 0 / 1 / 3 Myr for baseline simulations of an North PLD trough characterized by T_{sav} = 162 K upon the EWF wall and T_{sav} = 160 K upon the PWF wall. A total PLD thickness of Z = 2 km is assumed.

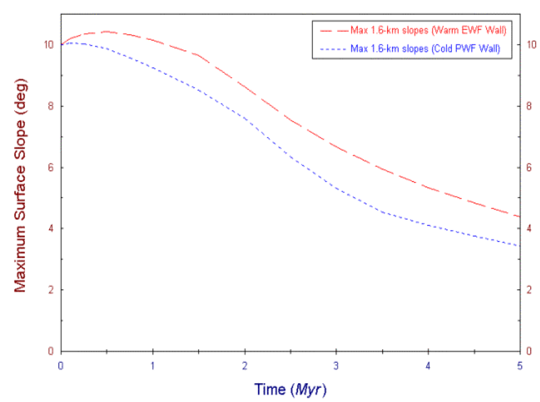

***Fig.** 5*. Temporal dependence of maximum 1.6-km surface slopes for both EWF and PWF trough walls, derived from baseline North PLD trough simulations for differential thermal conditions shown in Fig. 4.